

Steroid-resistant nephrotic syndrome and congenital anomalies of kidneys: Evidence of locus on chromosome 13q

ABHAY N. VATS, CHANDRA ISHWAD, KALYANI R. VATS, MICHAEL MORITZ, DEMETRIUS ELLIS, CHRISTINE MUELLER, URVASHI SURTI, MARIA Z. PARIZHSKAYA, MANUEL P. MEZA, LEAH BURKE, FRANCIS X. SCHNECK, MALIKA SAXENA, and ROBERT FERRELL

Department of Pediatrics, Children's Hospital of Pittsburgh, University of Pittsburgh School of Medicine, Pittsburgh, Pennsylvania; Department of Human Genetics, Graduate School of Public Health, University of Pittsburgh, Pittsburgh, Pennsylvania; Department of Reproductive Biology, Magee Women's Hospital, University of Pittsburgh School of Medicine, Pittsburgh, Pennsylvania; Department of Pathology, Magee Women's Hospital, University of Pittsburgh School of Medicine, Pittsburgh, Pennsylvania; Department of Pathology, Children's Hospital of Pittsburgh, University of Pittsburgh School of Medicine, Pittsburgh, Pennsylvania; Department of Radiology, Children's Hospital of Pittsburgh, University of Pittsburgh School of Medicine, Pittsburgh, Pennsylvania; Division of Medical Genetics, Department of Pediatrics, University of Vermont College of Medicine, Burlington, Vermont; and Department of Urology, Children's Hospital of Pittsburgh, University of Pittsburgh School of Medicine, Pittsburgh, Pennsylvania

Steroid-resistant nephrotic syndrome and congenital anomalies of kidneys: Evidence of locus on chromosome 13q.

Background. Steroid-resistant nephrotic syndrome (SRNS) and congenital anomalies of kidney and urinary tract (CAKUT) are major causes of renal dysfunction in children. Although a few patients with 13q deletion have been previously reported with renal anomalies, the association of SRNS with 13q has not been reported and critical regions associated with CAKUT have not been identified. We present the results of deletion mapping studies to identify the critical regions.

Methods. Cytogenetic and deletion mapping studies were performed on DNA obtained from peripheral blood of two children with renal anomalies and interstitial deletion of 13q as well as their parents. Twenty eight microsatellite markers with a spacing of 1–8 Mb (1–3 cM) were utilized.

Results. The patients (both males, 5 and 10 years old) had varying severity of developmental delay and other neurologic disorders. The renal involvement included hydronephrosis, ureterocele, renal dysplasia, and mesangioproliferative SRNS. Our studies imply existence of at least two critical regions in the 13q area that are linked to CAKUT. The first is a 7 Mb region defined by markers D13S776 and D13S891 shared by both patients. The second is a much larger region extending at least 33 Mb above D13S776 seen in one patient with severe renal malformations and SRNS.

Conclusion. We report an association of chromosome 13q with CAKUT as well as SRNS. Our studies suggest the presence of more than one gene in this region that is likely to be involved in renal development and function.

Key words: 13q deletion, CAKUT, steroid-resistant nephrotic syndrome, renal anomalies, ureteropelvic junction obstruction.

Received for publication October 8, 2002
and in revised form December 11, 2002, and January 29, 2003
Accepted for publication February 28, 2003

© 2003 by the International Society of Nephrology

Congenital anomalies of the kidney and urinary tract (CAKUT) are a major cause of renal dysfunction in childhood and span a wide range of urinary system malformations, including ureteropelvic junction (UPJ) obstruction, vesicoureteral reflux (VUR), hypoplastic or multicystic dysplastic kidneys, and bladder outlet obstruction [1–4]. These anomalies often coexist (i.e., VUR can often be seen in the contralateral side of individuals with ureteral duplication, or renal dysplasia) [5, 6]. Many of these malformations also show familial clustering with variable penetrance [2, 7–10].

Although the etiology of CAKUT is probably multifactorial, it is likely that many of the CAKUT cases have a genetic cause. Recent studies have identified mutations in the several genes that are associated with CAKUT in humans [2, 11–16]. Additionally, there is now growing evidence different renal and urologic malformations may even be caused by mutations in the same gene(s) [2]. Besides CAKUT, another common kidney disease [i.e., nephrotic syndrome (NS)/focal segmental glomerulosclerosis (FSGS)] is increasingly thought to have a genetic basis and lately several genes have been identified [17–22]. All of these studies point to genetic heterogeneity of CAKUT and NS/FSGS, although none of the NS/FSGS genes are associated with CAKUT. We identified two children with 13q deletion who had a range of CAKUT with one child having steroid-resistant nephrotic syndrome (SRNS). Although cases of 13q deletion syndrome have been previously identified with renal malformations, its association with SRNS has not been reported and no information is available on the critical regions on 13q associated with renal development [23]. We de-

scribe the results of cytogenetic and molecular genetic studies to identify the critical region(s) on 13q associated with renal anomalies.

METHODS

The study was approved by the Human Rights Committee of the Children's Hospital of Pittsburgh (CHP) and informed consent was obtained from the parents of the children described in the study. We identified two children with 13q deletion and peripheral blood was obtained for the genetic studies. One of the patients attended the clinics at CHP and the other patient was identified through the Chromosomal Deletion Outreach Organization (www.chromodisorder.org). The patients were investigated by various radiologic and biochemical tests, including ultrasonography, vesicocystourethrography (VCUG), intravenous pyelography (IVP), computed tomography (CT), and magnetic resonance imaging (MRI).

Histologic and morphometric studies

Light microscopic, electron microscopic, and immunofluorescence studies were performed on the kidney tissue in case #1. For light microscopy, the kidney tissue was fixed in 10% neutral buffered formalin, embedded in paraffin, cut at 3 μm , and stained with hematoxylin and eosin (H&E), periodic-acid Schiff (PAS), and trichrome stains. For electron microscopy studies, the tissue was fixed in 4% paraformaldehyde/0.5% glutaraldehyde, and postfixed in 1% osmium tetroxide and embedded in Epon-Araldite. Immunoglobulins (IgG, IgA, and IgM), C3, C4, C1q, fibrin, and albumin antibodies were used for direct immunofluorescence studies. For morphometric studies, images of light microscopy sections were acquired digitally using a Nikon Diaphot (Melville, NY, USA) inverted microscope, with a 40 \times objective lens, equipped with a Carl Zeiss CCD video camera (Thornwood, NY, USA) and a dedicated IBM-PC-compatible computer (Dell, Round Rock, TX, USA) at a final magnification of 532 \times for a 72 dots per inch (dpi) resolution image. The final image had a pixel value of 0.495 μm and the whole image analysis system was calibrated with a slide micrometer (Fisher Scientific, Hanover Park, IL, USA). The glomerular tuft region for each glomerulus ($N = 6$) was manually outlined (also shown in Fig. 3c) and the glomerular area (GA) was calculated using Metamorph image analysis software program (Version 4.6r10, Universal Imaging Corporation, Downingtown, PA, USA). The mean glomerular area (MGA) was calculated by averaging the individual GA of each glomerular tuft. The mean glomerular volume was estimated by the Weibel-Gomez method by the formula:

$$\text{Mean glomerular volume} = \frac{1.38 \times (\text{MGA})^{(3/2)}}{1.01}$$

where 1.38 is the shape coefficient for a sphere and 1.01 is the variability coefficient, assuming a 10% coefficient of variation [24–26].

Cytogenetic studies

These were performed on peripheral blood lymphocytes from the proband and the parents using standard protocols as previously described [27]. Studies included GTG banding and fluorescent in situ hybridization (FISH) using RB-1 and 13q34-qter specific (D13S327) probes in one patient.

Deletion mapping

Genomic DNA was extracted from peripheral blood lymphocytes by proteinase K digestion and phenol-chloroform extraction [22]. The two families were assessed for deletion mapping at 13q by microsatellite analysis. Twenty eight microsatellite markers spanning the 13q region were examined. Primer pairs were obtained commercially (Research Genetics, Huntsville, AL, USA). Microsatellite markers were analyzed after amplification by polymerase chain reaction (PCR). The PCR reactions were performed as described previously [28]. PCR products were diluted 1:1 with loading buffer [95% deionized formamide, 20 mmol/L ethylenediaminetetraacetic acid (EDTA), 0.025% xylene cyanol, and 0.025% bromophenol blue] heat-denatured and electrophoresed through 7% polyacrylamide gel containing 5.6 mol/L urea and 32% formamide for 3 hours at 55°C. Gels were exposed to x-ray films at -80°C . Genotypes were scored visually and deletion was mapped by comparing the genotypes of parents with that of the probands. The markers used were D13S787, D13S1493, D13S894, D13S626, D13S784, D13S791, D13S889, D13S891, D13S318, D13S776, D13S800, D13S265, D13S281, D13S167, D13S793, D13S154, D13S1252, D13S159, D13S779, D13S1267, D13S317, D13S174, D13S280, D13S1311, D13S796, D13S286, D13S895, and D13S285.

RESULTS

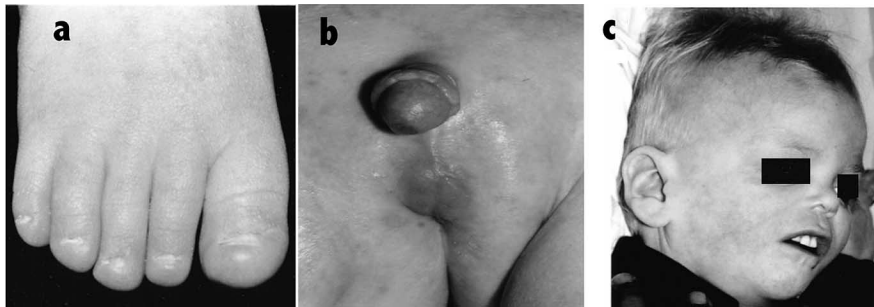
Table 1 shows a summary of findings in the two children. Case #1 had the more severe involvement with CAKUT as well as SRNS. Both the children had other significant organ involvement, including developmental delay.

Case #1

This boy was diagnosed with 13q deletion soon after birth and belonged to a large 53-member three-generation family with multiple members having rectourogenital malformations (including omphalocele, exstrophy, hypospadias, and cryptorchidism) and dysplastic nevus syndrome. The child presented with mild intermittent edema along with recurrent urinary tract infections at 3 years of age in 1999. He also had hypospadias and poorly

Table 1. Salient features of cases with 13q deletion

| Case No. | Current age years | Gender | Age at diagnosis | Karyotype | Renal abnormalities | Other abnormalities |
|----------|-------------------|--------|------------------|----------------------------|---|--|
| 1 | 5 | Male | At birth | 46, XY, del (13)(q12q22.3) | Bilateral ureterocele, right hydronephrosis bladder diverticulum, hyperechoic kidneys, steroid-resistant nephrotic syndrome | Bifid scrotum, hypospadias retinoblastoma, communicating hydrocephalus, mitral stenosis, cardiomyopathy, developmental delay, cleft soft palate, constipation, hypoplastic nails |
| 2 | 10 | Male | 1 year | 46, XY, del (13)(q21q32) | Right hydronephrosis, ureteropelvic junction obstruction, s/p pyeloplasty | Mental retardation, hypotonia apraxia, seizure, moderate bilateral hearing loss, excessive drooling, incontinence |

**Fig. 1.** Clinical features of case #1 showing (a) hypoplastic nails, (b) bifid scrotum and hypospadias, and (c) midfacial hypoplasia.

developed bifid scrotum (Fig. 1). Urinalysis at 3 years of age showed 3 to 4+ proteinuria, with serum albumin of 2.1 g/dL and hypercholesterolemia (251 mg/dL). He had normal serum creatinine (0.2 mg/dL), blood urea nitrogen (BUN) (7 mg/dL), and electrolytes (sodium, 142 mEq/L; potassium, 3.7 mEq/L; chloride, 103 mEq/L). A VCUG showed bilateral ureterocele with bladder diverticulum and no reflux (Fig. 2 a to c). A renal ultrasound showed bilateral hyperechoic hypoplastic kidneys and right-sided hydronephrosis (Fig. 2 d and e). He responded only partially to a prolonged course of steroids (prednisone 2 mg/kg/day orally for 8 weeks) with improvement in serum albumin (3.1 g/dL) but had no change in proteinuria (3 to 4+ during the whole 8-week course). He, however, showed a dramatic response to angiotensin-converting enzyme (ACE) inhibitor therapy. He responded completely to captopril therapy with normalization of serum albumin (4.4 g/dL) and complete disappearance of proteinuria. Withdrawal of captopril led to relapse and remission followed by reintroduction of captopril. However, prolonged captopril therapy was associated with development of hyponatremia and he was switched to losartan (Cozaar) therapy. He was maintained on low-dose losartan (6.25 mg/day orally) intermittently for 2 years. Extrarenal involvement in this child included bilateral retinoblastoma, communicating hydrocephalus (on MRI), severe mental retardation, gastroesophageal reflux, severe constipation, hypoplastic nails, and midfacial hypoplasia (Fig. 1). At approximately 5 years of age he was found to have polyvalvular heart disease, including mitral stenosis and a cardiomyopathy, even though an echocardiogram performed at 4

years of age, more than 1 year after the onset of SRNS, was considered to be normal. The hypertrophic and restrictive cardiomyopathy progressed very rapidly and he died at the age of 5 years 11 months due to complications related to mitral valve stenosis, pulmonary edema, and occult sepsis. A postmortem percutaneous kidney biopsy was performed within 2 hours of death.

Case #2

This 10-year-old boy presented with developmental delay and hypotonia at 1 year of age in Finland. Investigation performed at that stage showed right-sided hydronephrosis on ultrasonography. An IVP and diuresis renogram suggested UPJ obstruction on the right side. A right pyeloplasty was performed at 18 months of age. There have been no urinary or abdominal symptoms since then. Urinalysis at 8 years of age (in year 2000) showed microscopic hematuria with three to five red blood cells per high power field and no proteinuria. Other studies done at that time showed that BUN was 11 mg/dL, creatinine was 0.3 mg/dL, albumin was 4.6 g/dL, sodium was 138 mEq/L, potassium was 3.9 mEq/L, chloride was 101 mEq/L, and total carbon dioxide was 24 mEq/L. Extrarenal involvement in this patient included moderate bilateral hearing loss, apraxia, incontinence, mental retardation, epilepsy, and excessive drooling.

Histologic and morphometric studies

The postmortem kidney biopsy in case #1 showed enlarged glomeruli with dilated capillaries, expanded mesangial matrix, and increased mesangial cellularity. The degree of mesangial matrix expansion and mesangial

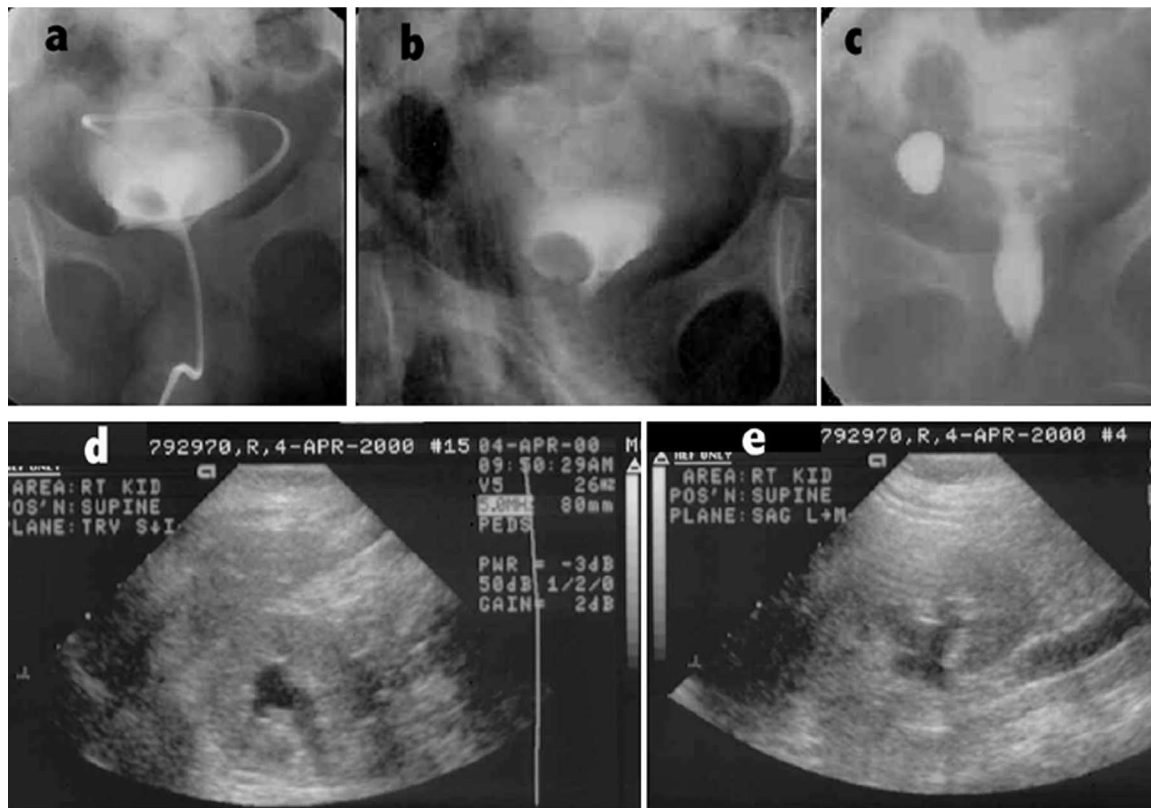


Fig. 2. Radiographic findings in case #1. Retrograde cystography showing a large right-sided and a smaller left-sided ureterocele seen as filling defects on initial filling phase (a), and voiding phase of the study (b). Post void film in (c) shows a bladder diverticulum on the right side. Renal ultrasound findings of the right kidney in the same patient showing a hyperechoic kidney with poor corticomedullary differentiation and minimal hydronephrosis in transverse (d) and sagittal (e) views.

cellularity varied between glomeruli (Fig. 3 a to d). Other glomerular changes included prominence of juxtaglomerular areas, hypertrophy of some visceral epithelial cells, as well as segmental parahilar sclerosis in two glomeruli (Fig. 3 b and c). Patchy interstitial fibrosis and tubular atrophy were also seen (Fig. 3d). Immunofluorescence studies revealed segmental, granular deposits of C3 and IgM in mesangial areas (Fig. 3 e and f). Electron microscopy studies showed expansion of mesangial matrix, increased numbers of mesangial cells, and a few small electron dense deposits in mesangium (Fig. 3 g and h). Although hypertrophy of visceral epithelial cells and microvillous transformation were observed, the foot process fusion was focal and mild (Fig. 3i). Morphometric studies were limited as only six glomeruli were present in the tissue submitted for light microscopy. The glomerular tuft area ranged from $1.1 \times 10^5 \mu\text{m}^2$ to $1.9 \times 10^5 \mu\text{m}^2$ and the mean glomerular volume was calculated to be $3 \times 10^6 \mu\text{m}^3$.

Cytogenetic studies

Karyotyping studies with GTG banding in case #1 showed interstitial 13q deletion [i.e., 46, XY, del(13)(q12q22.3)] (Fig. 4). FISH studies were performed in 10

metaphase cells. FISH with retinoblastoma gene probe (RB-1) which maps to 13q14 showed positive signals in only one chromosome 13. FISH with the 13q32-q33 specific (D13S585) and 13q34-qter specific (D13S327) probes showed positive signals in both 13 chromosomes, thus confirming the above findings. No cytogenetic abnormalities were found in the parents. Cytogenetic studies in case #2 showed interstitial deletion of 13q [i.e., 46, XY, del(13)(q21q32)]. No cytogenetic abnormalities were found in the parents of case #2.

Deletion mapping studies

Table 2 shows the details of deletion mapping studies. The PCR product sizes for each marker pair and the visually ascertained allele for each marker and each individual (arbitrarily labeled alphabetically) are shown. The physical distances for each marker are based on the June 2002 assembly of the human genome available through University of California Santa Cruz (UCSC) genome browser (<http://genome.ucsc.edu>). The genetic distances for the markers were derived from the genetic location database (LDB) (<ftp://cedar.genetics.soton.ac.uk/pub/chrom13/map.html>). Deletion mapping in case #1 showed a large deletion extending at least from 32 Mb to 73 Mb

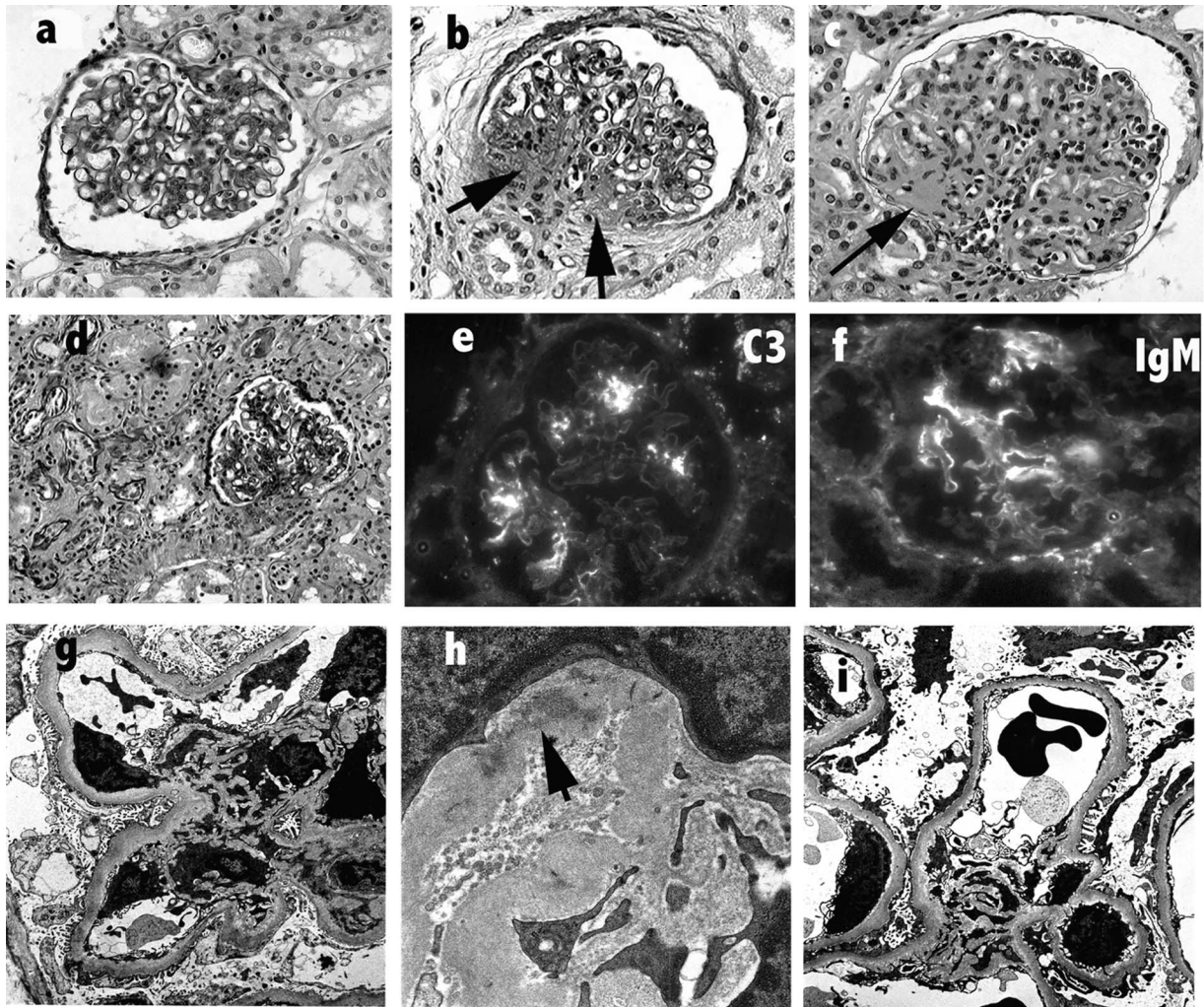


Fig. 3. Renal biopsy in case #1. (a) Light microscopy shows glomerulus with dilated capillaries and mild mesangial hypercellularity [periodic-acid Schiff (PAS) $\times 200$]. (b) Light microscopy shows glomerulus with perihilar sclerosis (arrows) (PAS $\times 200$). (c) Light microscopy shows enlarged glomerulus with mesangial hypercellularity and matrix expansion as well as perihilar sclerosis (arrow) [hematoxylin and eosin (H&E) $\times 400$]. The outlined tuft area was used to calculate glomerular area and volume. (d) Light microscopy of an area of tubular atrophy and a glomerulus with expanded mesangium. (e) Immunofluorescence microscopy shows segmental C3 deposits in mesangial areas. (f) Immunofluorescence segmental immunoglobulin M (IgM) deposits in mesangial areas. (g) Electron microscopy shows increased mesangial cellularity ($\times 6200$). (h) Electron microscopy shows few small electron dense deposits in mesangium (arrow) ($\times 34,000$). (i) Electron microscopy shows visceral epithelial cells (podocytes) with microvillous transformation and focal foot process fusion ($\times 6200$).

(25 cM to 73 cM). Deletion mapping in case #2 showed a smaller deletion extending at least from 65 Mb to 81 Mb (63 cM to 85 cM). The deleted region in both the cases is shown in bold.

Our studies imply existence of at least two critical regions in the 13q area that are involved in the development of CAKUT and SRNS. The first is a 7 Mb region defined by markers D13S776 and D13S891 and shared by both patients. The second is a much larger region extending at least 33 Mb above D13S776 seen in case #1.

DISCUSSION

SRNS and CAKUT are major causes for morbidity in pediatric age group and lately a number of studies have

focused on identification of genes responsible for these syndromes [2, 4]. Over the last two decades occasional cases of 13q deletion syndrome have been reported with CAKUT, but no information is available on the critical regions associated with renal development [23, 29, 30]. We report association of chromosome 13q with SRNS as well as CAKUT and provide evidence for location of at least two genes in this region that are likely to be responsible for renal development in utero and maintenance of glomerular permselectivity ex utero. Our studies suggest existence of two critical regions on 13q. The first is an at least 7 Mb region defined by markers D13S776 and D13S891 shared by both patients that is likely linked to CAKUT. The second is a much larger

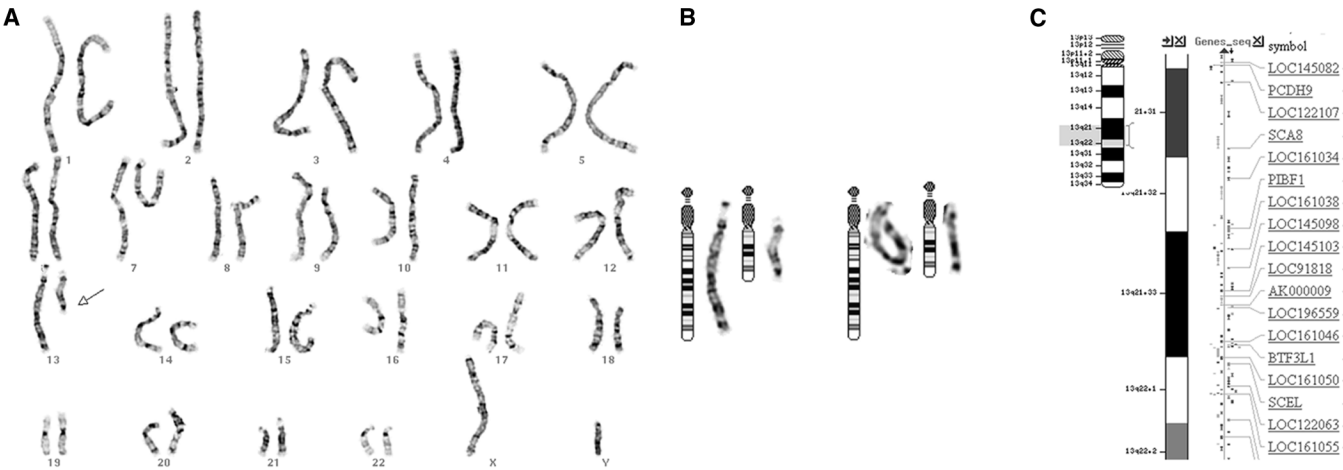


Fig. 4. Karyotype details of case #1. (A) Karyotype shows deleted 13q region (arrow). (B) The details of the deleted region in two of the cultured cells along with an ideogram of the region. (C) A schematic diagram of the deleted region of the chromosome common to both cases with some of the genes in the region displayed as symbols.

Table 2. Deletion mapping data for cases #1 and 2 and their parents

| Marker | Position Kb | Position cM | PCR product size bp | Annealing temperature used °C | Case 1 | Case 1 father | Case 1 mother | Case 2 | Case 2 father | Case 2 mother |
|----------|----------------|----------------|------------------------|-------------------------------------|--------|------------------|------------------|--------|------------------|------------------|
| D13S787 | 22360 | 7 | 251 | 56 | AB | AB | AA | BC | BC | BC |
| D13S1493 | 31995 | 25.8 | 250 | 57 | BB | BC | AB | AD | BD | AC |
| D13S894 | 36724 | 33 | 190 | 56 | BB | AB | BB | AB | AB | BB |
| D13S626 | 51310 | 56.77 | 339 | 55 | B | AC | BB | CD | CD | BD |
| D13S784 | 53073 | 57.06 | 195–196 | 55 | C | AB | BC | AA | AA | AA |
| D13S889 | 61530 | 60.43 | 294–295 | 55 | B | AC | BC | BC | BB | BC |
| D13S776 | 65395 | 67.58 | 142 | 55 | D | AC | BD | BB | AB | BC |
| D13S318 | 68543 | 65.23 | 284 | 51 | B | AD | BC | B | AA | BD |
| D13S800 | 71842 | 69.82 | 295–296 | 56 | C | AB | BC | D | BB | DD |
| D13S791 | 71842 | 72.57 | 293–294 | 58 | D | BC | AD | D | AC | BD |
| D13S891 | 72786 | 63.76 | 200 | 51 | A | BC | AB | AA | AB | AA |
| D13S317 | 80689 | 85.07 | 200 | 56 | AB | AC | BD | DD | CD | BD |
| D13S265 | 88733 | 86.56 | 293–294 | 58 | NA | NA | NA | BC | BC | BB |
| D13S281 | 92923 | 92.8 | 238 | 55 | NA | NA | NA | AC | AC | AA |
| D13S167 | 93035 | 92.6 | 184–192 | 55 | NA | NA | NA | CC | CC | CC |
| D13S154 | 94622 | 94.4 | 243–277 | 55 | NA | NA | NA | DE | EE | DG |
| D13S793 | 96311 | 95.75 | 262 | 57 | AA | AC | AB | AC | AC | AC |
| D13S1252 | 96897 | 96.1 | 194–238 | 62 | NA | NA | NA | AB | BB | AB |
| D13S159 | 97414 | 96.4 | 168–203 | 56 | NA | NA | NA | BB | BC | AB |
| D13S1267 | 99257 | 98.49 | 184–216 | 58 | AC | AB | BC | AB | AB | AB |
| D13S779 | 99864 | 98.64 | 191 | 52 | NA | NA | NA | AC | CC | AC |
| D13S174 | 101314 | 99.7 | 173–199 | 55 | NA | NA | NA | BD | AB | BD |
| D13S280 | 101907 | 100.14 | 138 | 55 | NA | NA | NA | AD | CD | AB |
| D13S1311 | 104552 | 102.13 | 141–149 | 62 | NA | NA | NA | BC | CC | BC |
| D13S286 | 105297 | 102.59 | 175–195 | 56 | NA | NA | NA | BC | BB | AC |
| D13S796 | 106249 | 104.5 | 167 | 56 | CD | AC | BD | CC | BC | CC |
| D13S895 | 107948 | 111.8 | 160 | 56 | AC | AB | CD | AB | AB | BB |
| D13S285 | 111405 | 113.58 | 92–106 | 56 | NA | NA | NA | BE | BG | EG |

region, extending at least 33 Mb above D13S776, seen in case #1, and we propose that it contains a gene that is linked to SRNS.

To our knowledge, chromosome 13q has not so far been associated with SRNS phenotype and we report this association for the first time. Case #1 presented with insidious-onset NS that was refractory to a long course

of steroids. Postmortem kidney biopsy provided further insight into the pathology of 13q-associated SRNS. The biopsy revealed well-formed glomeruli and tubules as well as absence of dysplastic features. The biopsy findings were compatible with mesangioproliferative glomerulopathy with possible progression to FSGS. The mean glomerular volume estimate, although limited by the small

number of glomeruli studied, also served to confirm the visual impression of glomerular hypertrophy. The mean glomerular volume of $3 \times 10^6 \mu\text{m}^3$ in case #1 was considerably higher (by almost three times) than seen in age-matched minimal-change disease and normal controls in our previous studies on these patient groups (abstract; Vats A, et al, *J Am Soc Nephrol* 5:797, 1994). To put it in perspective, in our studies on congenital NS patients, the mean glomerular volume was found to be $1.4 \times 10^6 \mu\text{m}^3$ (range, 0.5 to $3.6 \times 10^6 \mu\text{m}^3$), and that of age-matched minimal-change NS patients was $0.7 \times 10^6 \mu\text{m}^3$ (range, 0.4 to $0.9 \times 10^6 \mu\text{m}^3$) [26]. Mesangioproliferative glomerulopathy and glomerulomegaly, however, are not unique to 13q-associated SRNS and may be seen in several other proteinuric states that can be either idiopathic or secondary to a number of conditions, including congenital heart disease [31]. In case #1, the biopsy was taken later in the course of the illness, when the patient already had end-stage heart disease. Although it is possible that his cardiac decompensation may have contributed to the renal pathology, the SRNS was most likely a primary condition as it preceded the onset of cardiomyopathy by almost 2 years. Thus, the 13q-associated SRNS is a nonminimal change process and can be associated with a mesangioproliferative and segmentally sclerosing glomerulopathy.

Recently several genes, located on various chromosomes (i.e., 19q13 [nephrin (*NPHS1*) and alpha actinin 4 (*ACTN4*)], and 1q25 [podocin (*NPHS2*)] have been associated with SRNS/FSGS [18–22, 32]. Also two genes on chromosome 11 [i.e., the Wilms tumor-1 (*WT-1*) and another gene tentatively labeled *FSGS2*] have been linked to SRNS/FSGS [14, 21]. Interestingly, *WT-1*, located at 11p13, is associated with a phenotype with some similarities to the features seen in case #1 (i.e., diffuse mesangial sclerosis and SRNS as well as urologic malformations) [14]. SRNS is, thus, a genetically heterogeneous disease [32], and our studies provide evidence for another SRNS-associated gene located in the 13q region. Interestingly, there were several other family members with urogenital malformations on the maternal side of the case #1 family. However the parental chromosomal assessment, by karyotyping, was normal. We propose that the *SRNS* gene on 13q is extremely responsive to ACE inhibitors, and to angiotensin receptor blockade (ARB). Since the renin-angiotensin system manipulation, by ACE inhibitors and/or ARB, is an important therapeutic tool in the management of various proteinuric states, our studies may provide clues to location of gene(s) that are important in mediating the renoprotective effects of these agents. The critical region for this gene is fairly large (i.e., at least 33 Mb approximately), but contains several interesting genes, including human proto-oncogene *c-fms* (*FMS*)-related tyrosine kinase-1 (*FLT-1*). *FLT-1* is also called vascular endothelial growth factor

receptor 1 and is expressed in endothelial cells. This gene is located above the retinoblastoma (*Rb*) gene locus at 13q14 [33]. Identification of additional 13q-linked SRNS cases and narrowing of the region would, however, be required to allow any further discussion of positional candidate genes.

Although the 13q deletion in case #1 is fairly large, the deleted region shared by both patients is smaller, extending at least 7 Mb (7 cM), and is likely to contain a CAKUT-associated gene. However, since the deletion can extend further telomeric to D13S891 in case #1, this shared area can potentially be larger. It is interesting to note that both the patients were males and had deletions of paternal alleles. As only two patients are described in our studies, we cannot make any further generalizations on the significance of these observations; however, future studies may identify the role of gender and genomic imprinting, if any, in the causation of 13q-associated CAKUT. Recently, several genes responsible for CAKUT have been identified in humans and animal models, but none lie on chromosome 13q [11–16]. An examination of the 7 Mb minimal critical region, shared by the two cases, reveals a number of characterized genes such as protocadherin 9 (*PCDH9*), the human homolog of *Drosophila* dachshund gene (*DACH*), and basic transcription factor 3-like 1 (*BTF3L1*), as well as a number of computer-predicted genes. Of these genes, *DACH* is a strong candidate gene as it is expressed in developing eyes, kidneys, ears, and limbs and interacts with the eyes absent gene (*EYA*), which is associated with branchio-oto-renal (BOR) syndrome in humans [34]. Also, *BTF3L1*, a transcription factor-like gene whose function is unknown at present, and *PCDH9*, an adhesion molecule, may be a good candidate genes. One or more of these genes may need to be investigated upon completion of further gene localization studies.

Finally, the CAKUT and SRNS-associated critical regions we described lie significantly centromeric to 13q regions reported in previous such associations (usually around 13q32-q33), although at least one patient with del(13)(q14.3q22) was reported with unilateral renal agenesis [23, 29, 30, 35]. Indeed, in a series of 22 retinoblastoma patients, with deletions in the proximal 13q regions, no renal or urinary findings were reported [36]. In view of the silent and asymptomatic nature of many renal diseases, our findings would suggest that a careful assessment of renal function and structure in cases with 13q deletion is appropriate. Institution of such assessment, including yearly urinalysis, may uncover additional patients with renal involvement and may aid gene localization studies in future.

CONCLUSION

We report association of interstitial deletion of 13q with steroid-resistant proteinuria and CAKUT and pro-

vide evidence for two critical regions. We also recommend that patients with similar deletions be assessed for renal involvement. It is anticipated that further gene localization studies in this region, both in humans and animal models, would lead to identification of additional genes involved in the complex ontogeny of the excretory system.

ACKNOWLEDGMENTS

We are grateful to the children described in the report and their parents for their support and help. We thank Linda Sorg from Chromosome Deletion Outreach for her help in identification of 13q deletion patients. This study was supported by a Young Investigator Award from the National Kidney Foundation and a K23 award from NIH (DK02854) to Dr Abhay Vats.

We are currently enrolling additional patients with 13q deletion in our gene mapping studies and would appreciate contact from the parents and caregivers of other children with 13q deletions by phone (+1 412 692 5182) or e-mail (abhay.vats@chp.edu).

Finally, it is acknowledged that Dr. Abhay Vats is a consultant for ViraCor Biotechnologies, Lee's Summit, MO.

Reprint requests to Abhay N. Vats, M.D., Department of Pediatrics, Division of Pediatric Nephrology, Children's Hospital of Pittsburgh, 3705 Fifth Avenue, Pittsburgh, PA 15213.
E-mail: abhay.vats@chp.edu

REFERENCES

- WARADY BA, HEBERT D, SULLIVAN EK, *et al*: Renal transplantation, chronic dialysis, and chronic renal insufficiency in children and adolescents. The 1995 Annual Report of the North American Pediatric Renal Transplant Cooperative Study. *Pediatr Nephrol* 11:49–64, 1997
- ICHIKAWA I, KUWAYAMA F, POPE JC, IV, *et al*: Paradigm shift from classic anatomic theories to contemporary cell biological views of CAKUT. *Kidney Int* 61:889–898, 2002
- BROWN T, MANDELL J, LEBOWITZ RL: Neonatal hydronephrosis in the era of sonography. *Am J Roentgenol* 61:959–963, 1987
- POPE JC, IV, BROCK JW, III, ADAMS MC, *et al*: How they begin and how they end: Classic and new theories for the development and deterioration of congenital anomalies of the kidney and urinary tract. CAKUT. *J Am Soc Nephrol* 61:2018–2028, 1999
- HINCHLIFFE SA, CHAN YF, JONES H, *et al*: Renal hypoplasia and postnatally acquired cortical loss in children with vesicoureteral reflux. *Pediatr Nephrol* 6:439–444, 1992
- ATIEH B, HUSMANN D, BAUM M: Contralateral renal anomalies in multicystic dysplastic kidney disease. *J Pediatr* 61:65–67, 1992
- ROODHOOF A, BIRNHOLZ J, HOLMES L: Familial nature of congenital absence and severe dysgenesis of both kidneys. *N Engl J Med* 310:1341–1345, 1984
- MURUGASU B, COLE B, HAWKINS E, *et al*: Familial renal adysplasia. *Am J Kidney Dis* 4:490–494, 1995
- IZQUIERDO L, PORTEOUS M, PARAMO P, *et al*: Evidence for genetic heterogeneity in hereditary hydronephrosis caused by pelviureteric junction obstruction, with one locus assigned to chromosome 6p. *Hum Genet* 89:557–560, 1992
- WOOLF A, WINNYARD P: Advances in the cell biology and genetics of human kidney malformations. *J Am Soc Nephrol* 9:1114–1125, 1998
- SANYANUSIN P, SCHIMMENTI LA, MCNOE LA, *et al*: Mutation of the PAX2 gene in a family with optic nerve colobomas, renal anomalies and vesicoureteral reflux. *Nat Genet* 61:358–363, 1995
- ABDELHAK S, KALATZIS V, HEILIG R, *et al*: A human homologue of the Drosophila eyes absent gene underlies branchio-oto-renal (BOR) syndrome and identifies a novel gene family. *Nat Genet* 61:157–164, 1997
- VAN ESCH H, GROENEN P, NESBIT MA, *et al*: GATA3 haplo-insufficiency causes human HDR syndrome. *Nature* 406:419–422, 2000
- SCHUMACHER V, SCHVER K, WULH E, *et al*: Spectrum of early onset nephrotic syndrome with WT1 missense mutations. *Kidney Int* 53:1594–1600, 1998
- NISHIMURA H, YERKES E, HOHENFELLNER K, *et al*: Role of the angiotensin type 2 receptor gene in congenital anomalies of the kidney and urinary tract, CAKUT, of mice and men. *Mol Cell* 61:1–10, 1999
- HIRAOKA M, TANIGUCHI T, NAKAI H, *et al*: No evidence for AT2 gene derangement in human urinary tract anomalies. *Kidney Int* 61:1244–1249, 2001
- HABIB R: Focal glomerular sclerosis. *Kidney Int* 4:355–361, 1973
- LENKKERI U, MANNIKKO M, MCCREADY P, *et al*: Structure of the gene for congenital nephrotic syndrome of the Finnish type (NPHS1) and characterization of mutations. *Am J Human Genet* 64:51–61, 1999
- KAPLAN JM, KIM SH, NORTH KN, *et al*: Mutations in ACTN4, encoding alpha-actinin-4, cause familial focal segmental glomerulosclerosis. *Nat Genet* 24:251–256, 2000
- BOUTE N, GRIBOUVAL O, ROSELLI S, *et al*: NPHS2, encoding the glomerular protein podocin, is mutated in autosomal recessive steroid-resistant nephrotic syndrome. *Nat Genet* 24:349–354, 2000
- WINN MP, CONLON PJ, LYNN KL, *et al*: Linkage of a gene causing familial focal segmental glomerulosclerosis to chromosome 11 and further evidence of genetic heterogeneity. *Genomics* 58:113–120, 1999
- VATS A, NAYAK A, ELLIS D, *et al*: Familial nephrotic syndrome: Clinical spectrum and linkage to chromosome 19q13. *Kidney Int* 57:875–881, 2000
- BROWN S, GERSEN S, ANYANE-YEBOA K, WARBURTON D: Preliminary definition of a “critical region” of chromosome 13 in q 32: Report of 14 cases with 13q deletions and review of the literature. *Am J Med Gen* 45:52–59, 1993
- LANE PH, STEFFES MW, MAUER SM: Estimation of glomerular volume: A comparison of four methods. *Kidney Int* 41:1085–1089, 1992
- WEIBEL ER, GOMEZ DM: A principle for counting tissue structures on random sections. *J Appl Physiol* 17:343–348, 1962
- VATS A, COSTELLO B, MAUER M: Glomerular structural factors in progression of congenital nephrotic syndrome. *Pediatr Nephrol* 18:234–240, 2003
- MCPHERSON EW, LANERI G, CLEMENS MM, *et al*: Apparently balanced t(1;7)(q21.3;q34) in an infant with Coffin-Siris syndrome. *Am J Med Genet* 71:430–433, 1997
- ISHWAD CS, FERRELL RE, ROSSIE KM, *et al*: Loss of heterozygosity of the short arm of chromosomes 3 and 9 in oral cancer. *Int J Cancer* 69:1–4, 1996
- BENN PA, WARBURTON D, BYRNE MJ, *et al*: A fetus with a chromosome 13 ring placenta with chromosome 13 rod/ring mosaicism. *Prenat Diag* 3:297–302, 1983
- KUHNLE U, BARTSCH O, WERNER W, SCHUSTER T: Penoscrotal inversion, hypospadias, imperforate anus, facial anomalies, and developmental delay: Definition of a new clinical syndrome. *Pediatr Surg Int* 16:396–399, 2000
- HIDA K, WADA J, YAMASAKI H, *et al*: Cyanotic congenital heart disease associated with glomerulomegaly and focal segmental glomerulosclerosis: Remission of nephrotic syndrome with angiotensin converting enzyme inhibitor. *Nephrol Dial Transplant* 17:144–147, 2002
- POLLAK MR: Inherited podocytopathies: FSGS and nephrotic syndrome from a genetic viewpoint. *J Am Soc Nephrol* 13:3016–3023, 2002
- IMBERT A, ROSNET O, MARCHETTO S, *et al*: Characterization of a yeast artificial chromosome from human chromosome band 13q12 containing the FLT1 and FLT3 receptor-type tyrosine kinase genes. *Cytogenet Cell Genet* 67:175–177, 1994
- IKEDA K, WATANABE Y, OHTO H, KAWAKAMI K: Molecular interaction and synergistic activation of a promoter by Six, Eya, and Dach proteins mediated through CREB binding protein. *Mol Cell Biol* 22:6759–6766, 2002
- BROWN SA, WARBURTON D, BROWN LY, *et al*: Holoprosencephaly due to mutations in ZIC2, a homologue of Drosophila odd-paired. *Nat Genet* 20:180–183, 1998
- BAUD O, CORMIER-DAIRE V, LYONNET S, *et al*: Dysmorphic phenotype and neurological impairment in 22 retinoblastoma patients with constitutional cytogenic 13q deletion. *Clin Genet* 55:478–482, 1999